Journal of Alloys and Compounds 502 (2010) 74–79

Contents lists available at ScienceDirect

Journal of Alloys and Compounds

journal homepage: www.elsevier.com/locate/jallcom

Effects of Fe addition and addition sequence on carbon inoculation of Mg–3%Al alloy

Jun Du*, Minghua Wang, Wenfang Li

School of Materials Science and Engineering, South China University of Technology, Guangzhou 510640, China

ARTICLE INFO

Article history:
Received 22 January 2010
Received in revised form 20 April 2010
Accepted 23 April 2010
Available online 4 May 2010

Keywords:
Mg–Al alloy
Grain refinement
Nucleating substrate
Iron
Carbon

ABSTRACT

The Mg–3%Al melt was treated by carbon inoculation and/or Fe addition. The effects of Fe addition and addition sequence on the carbon inoculation of Mg–3%Al alloy were investigated in the present study. The role of Fe in the grain refinement of Mg–3%Al alloy treated by carbon inoculation was closely associated with the operating sequence of carbon inoculation and Fe addition. Fe has no obvious effect on the grain refinement of Mg–3%Al alloy by carbon inoculation under the condition that Fe pre-existed in the Mg–3%Al melt before carbon inoculation. However, Fe played an inhibiting role under the condition that the Mg–3%Al melt had been inoculated by carbon before Fe addition. The Al–C–O particles were observed in the sample treated only by carbon inoculation. In addition to Al–C–O particles, Al–C–O–Fe particles could be observed in the sample treated by Fe addition and then carbon inoculation. These Al–C–O and Al–C–O–Fe particles, actually being Al–C and Al–C–Fe phases, should be the potent nucleating substrates for Mg grains, resulting in the grain refinement. However, the Al–C–O–Fe-rich intermetallic particles were mainly observed in the samples treated by carbon inoculation and then Fe addition. The Al–C–O–Fe particles, actually being Al–C–Fe phases, formed under this condition should not be the potent nucleating substrates for Mg grains, resulting in the grain coarsening.

1. Introduction

During the past two decades, the consumption of magnesium alloys has steadily increased in the industries of electronics and automobile parts since magnesium is the lightest structural metal currently available in the world [1–3]. Among a broad range of magnesium alloys, Mg–Al type alloys take a dominant position in the magnesium products [1–3]. The grain refinement has been proved to be a very effective route to improve the mechanical properties of the Mg–Al type alloys [4–6]. Many grain refining methods have been developed, such as addition of solute elements [4,7,8], superheating [7–10], $FeCl_3$ inoculation [11] and carbon inoculation [5–8,12–19]. Among them, the carbon inoculation offers many practical advantages, like the lower cost, the lower operating temperature and the less fading [7,8]. The refining mechanism of the carbon inoculation firstly proposed by Emley in his book [20] is that the Al_4C_3 particles formed in the Mg–Al melt act as nucleating substrates for Mg grains during solidification. This hypothesis has been widely appreciated to date by many researchers [5–10,12–18].

The element of Fe was proved to be an important factor to determine the refining efficiency for the Mg–Al alloys refined by carbon inoculation [21–24]. Discrepant results that whether Fe inhibits the grain refinement or not were obtained by some researchers [21–24]. Haitani et al. [21] concluded firstly that Fe was an inhibiting element for grain refinement, since it poisoned the potency of the Al_4C_3 nucleating particles by transforming Al_4C_3 into Al–C–Fe-rich intermetallic compounds. From then on, this viewpoint was widely accepted by many researchers [7,8,10,22]. However, Pan et al. [23] insisted that Fe played a positive role in the formation of the nucleating particle rather than an inhibiting element. The same result was also obtained in the authors' previous study [24]. In these studies, the Al–C–Fe-rich intermetallic particles were also observed. However, these Al–C–Fe-rich particles acted as nucleating substrates for Mg grains resulting in the grain refinement [23,24]. It is difficult to understand clearly why contradictory conclusions were made for the same phenomenon. The exact mechanism is not disclosed yet.

It should be noted that the ultra-high purity raw materials, having very low content of Fe (<10 ppm), were used in the studies performed by Haitani and Cao et al. [21,22]. However, the commercial raw materials with relatively high content of Fe (0.05%) were employed by Pan et al. [23]. In the authors' previous study [24], different Fe contents (from 0.05% to 0.5%) were added into the Mg–Al melt before being refined by carbon inoculation. As far as the ultra-high purity Mg–Al alloys are concerned, Cao et al. [22] found

* Corresponding author at: Department of Metallic Materials, School of Materials Science and Engineering, South China University of Technology, Wu Shan Road 381, Tian He District, Guangzhou 510640, China. Tel.: +86 20 8711 3747; fax: +86 20 8711 3747.
E-mail address: tandujun@sina.com (J. Du).

0925-8388/$ – see front matter © 2010 Elsevier B.V. All rights reserved.
doi:10.1016/j.jallcom.2010.04.156

they have native grain refinement due to the existence of native Al_4C_3 particles. In the Haitani's study [21], therefore, the native Al_4C_3 particles should pre-exist in the melt before Fe addition. On the contrary, the element Fe pre-existed in the Mg–Al melt before being refined by carbon inoculation in the studies performed by Pan and authors [23,24]. Therefore, it seems that whether Fe plays an inhibiting role or not in the grain refinement of Mg–Al alloys by carbon inoculation should be associated closely with the operating sequence of carbon inoculation and Fe addition.

This work aimed to study the effects of Fe addition and addition sequence on carbon inoculation of the Mg–3%Al alloy. Fe is an inevitable impurity element in the commercial Mg–Al alloys. From the viewpoint of commercial industries, such investigation has more practical significance, and also some important data can be provided to develop a suitable grain refiner, *i.e.* reliable and easy to be applied to Mg–Al alloys.

2. Experimental procedure

The raw materials used in the present study included relatively high purity magnesium (99.95%Mg, 0.002%Fe, 0.002%Mn), high purity aluminum (99.99%Al). The alloy used in the present study was Mg–3%Al alloy, which has the basic compositions widely used in industries as wrought magnesium alloy. To inoculate the Mg–Al melt, the pellets containing carbon powder were prepared beforehand. The details on the pellets have been described elsewhere [17,18].

The MgO crucible of relatively high purity was used in the present study to avoid the uptake of other impurity elements. The Mg–3%Al alloy of about 20 g was melted in an electric resistance furnace at 760 °C. To avoid oxidation, the melt was covered by a protective flux (45%$MgCl_2$, 35%KCl, 10%CaF_2, 10%NaCl (mass ratio)). The high purity Al–15%Fe master alloy was used to add Fe into Mg–Al melt. The addition amounts of Fe and carbon were 0.1% and 0.2% (mass ratio) of the melt, respectively. To exactly control the Al content in Mg–Al melt, the amounts of Al in the pellets and Al–15%Fe master alloy were taken into consideration.

Six samples were prepared in the present study. They were the sample of Mg–3%Al alloy without treatment and the two samples treated separately by carbon inoculation and Fe addition, as well as the three samples treated by the combination of carbon inoculation and Fe addition. The preparation details of the six samples, corresponding to the process Nos. 1–6, were described as following.

The pure Mg and pure Al were melted together and the melt was held for 20 min before being poured. This process route corresponded to process No.1 to prepare the sample without treatment. The pellets containing carbon powder were plunged into the Mg–Al melt. After that, the melt was held for 10 min, manually stirred for 1 min with a magnesia rod, and continued to be held for 10 min. This process route corresponded to process No. 2 to prepare the samp1e treated only by carbon inoculation. As for the process No. 3 to prepare the sample treated only by Fe addition, the pure Mg, pure Al and Al–15%Fe master alloy were melted together and the melt was held for 20 min before being poured.

The pure Mg, pure Al and Al–15%Fe master alloy were melted together, and then the melt containing 0.1%Fe was further treated by carbon inoculation, like as the process No. 2. This process route corresponded to the process No. 4. As for the process route No. 5, the Mg–Al melt was firstly treated by carbon inoculation, like as the process No. 2. After that, this Mg–Al melt was further treated by 0.1%Fe addition and was held for 10 min before being poured. The process No. 6 was almost the same as process No. 5. The carbon-inoculated melt further treated by 0.1%Fe addition was held for a longer time of 20 min before being poured.

For the samples prepared through process Nos. 4–6, they were all treated by the combination of carbon inoculation and Fe addition. However, the operating sequences of carbon inoculation and Fe addition were different. For the sample prepared through process No. 4, the Mg–Al melt was firstly treated by 0.1%Fe addition and then inoculated by carbon. The contrary sequence was carried out in process Nos. 5 and 6. The Mg–Al melt was firstly inoculated by carbon and then treated by 0.1%Fe addition.

The melts prepared through different process routes were poured into a cylindric iron-mould with the size of Ø20 mm × 25 mm, which was preheated at 500 °C. Metallographic samples were cut in the horizontal direction at the position of 10 mm from the bottom of the samples. To reveal the grain boundaries clearly, the samples were held at 420 °C for 6 h, and then were air-cooled. These heat-treated samples for grain morphology observation were prepared using a standard procedure. The grain microstructures were observed using the Leica DFC320 type optical microscope. Five pictures for every sample were taken from the central area of the metallographic sample. The grain size was evaluated using linear intercept method described in ASTM standard E112-88. The five data of grain sizes measured from five pictures were averaged. The average value and standard deviation were used to evaluate the grain size of every sample.

To observe the microstructural characteristics of nucleating particles in the samples, the as-cast samples etched with 2 vol.% nitride acid ethanol solution were further studied by Quanta 200 scanning electron microscope (SEM) equipped with IE350MT energy-dispersive X-ray (EDX) spectrometer.

3. Results

3.1. Grain refining efficiency

Fig. 1 shows the grain morphologies of the Mg–3%Al alloy treated through different process routes. These pictures were taken under relatively high magnification (100×). The pictures used to evaluate the grain sizes were taken under low magnification (50×) since more grains existed in the pictures. The grain sizes of the six samples are listed in Fig. 2. For the sample without treatment, the grain was coarse with a size of 610 ± 135 μm (Fig. 1a). The grain was significantly refined for the sample treated by carbon inoculation. Its grain size was decreased to 183 ± 25 μm (Fig. 1b). For the sample treated by 0.1%Fe addition, its grain size was about 525 ± 95 μm (Fig. 1c). For the sample treated through process No. 4, its grain size of 188 ± 31 μm was almost the same as the sample treated by only carbon inoculation. Compared to the samples treated through process Nos. 3 and 4, the grains became very coarse for the samples treated through process Nos. 5 and 6 (Fig. 1e and f). Their grain sizes were 582 ± 140 and 708 ± 165 μm, respectively.

Obviously, Fe had no effect on the grain refinement of the Mg–3%Al alloy by carbon inoculation under the condition that Fe pre-existed in the Mg–Al melt. On the contrary, Fe played an inhibiting role in the grain refinement of the Mg–3%Al alloy if the Mg–Al melt had already been treated by carbon inoculation before Fe was added. Consequently, a conclusion could be drawn that the effect of Fe on grain refinement of Mg–Al alloys by carbon inoculation was closely associated with the operating sequence of carbon inoculation and Fe addition.

3.2. SEM observations

By SEM observation, the Al–C–O particles were easily captured in the sample treated by carbon inoculation. The sizes of these particles distributed in the range between about 0.4 and 3 μm. Fig. 3 shows the typical images of the Al–C–O particles. The particles denoted by A to C were all Al–C–O particles, and their typical EDS spectra measured from the particles denoted by A and B are also illustrated in Fig. 3.

Judged by EDS spectra, two kinds of particles could be observed in the sample treated through process No. 4. They were Al–C–O and Al–C–O–Fe particles. Fig. 4 shows the typical images of the particles existing in this sample. The particle denoted by A was Al–C–O–Fe particle and the other particles denoted by B to D were all Al–C–O particles. The sizes of these particles distributed in the range between about 1.5 and 3 μm. The particles with a size of less than 1 μm were hardly observed.

As for the two samples treated through process Nos. 5 and 6, many intermetallic particles could be also easily observed. These particles were mainly Al–C–O–Fe particles, while the Al–C–O particles were hardly found. The images of the Al–C–O–Fe particles and their typical EDS spectra are shown in Figs. 5 and 6. The sizes of the particles existing in these two samples were obviously larger than those in the samples treated through process Nos. 2 and 3. The size distributions of the particles existing in these two samples were both in the range between about 2 and 10 μm. Compared to the sample treated through process No. 5, more particles with a larger size could be found in the sample treated through process No. 6. Judged by EDS spectra, the Al–C–O–Fe particles in these two samples could be classified into two types. One type was that the particles contained low content of Fe, such as the particles denoted by A in both Figs. 5 and 6. The other type was that the particles contained high content of Fe, such as the particles denoted by B in both Figs. 5 and 6.

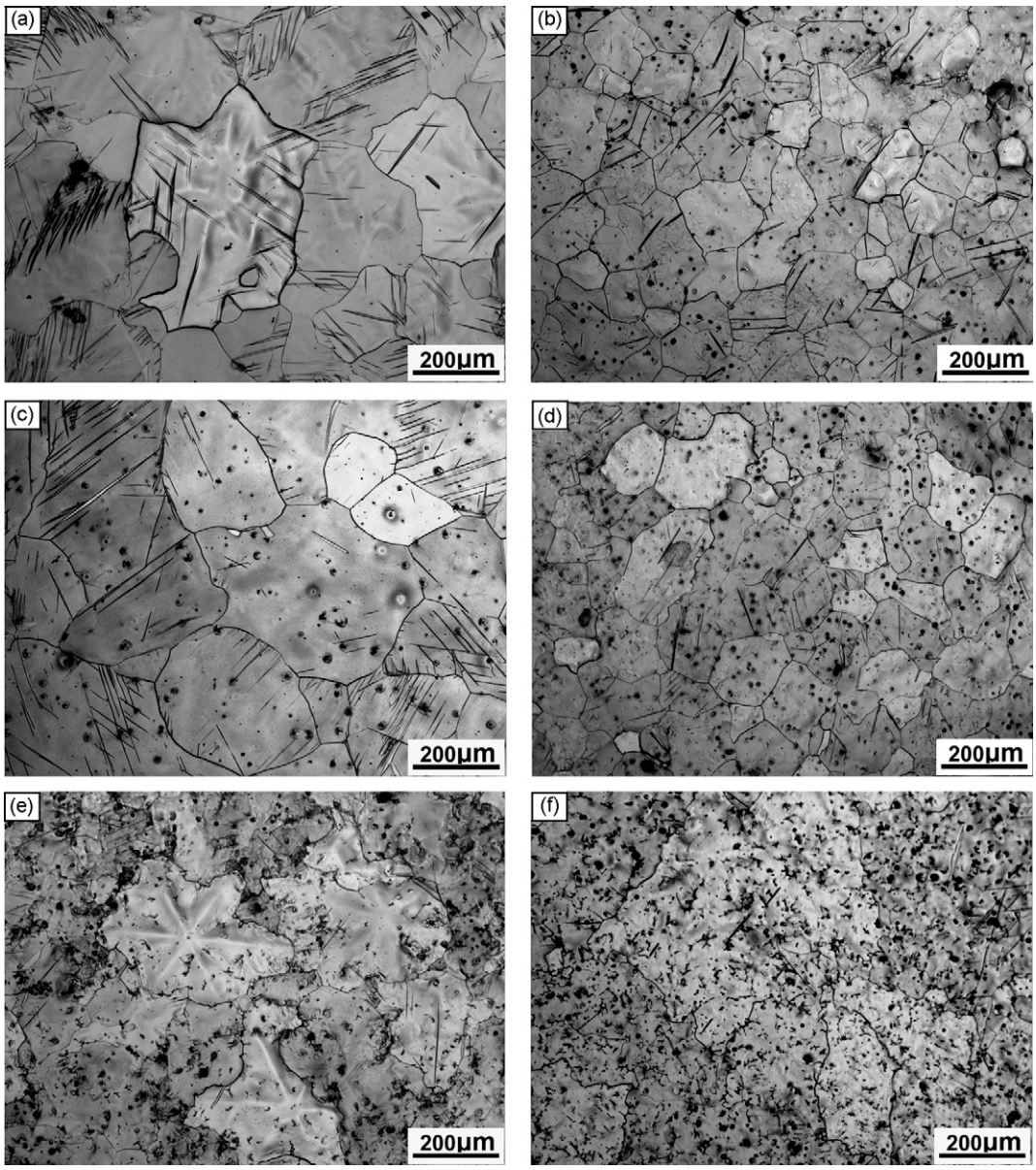

Fig. 1. Grain morphologies of the Mg–3%Al alloy without treatment (a) and treated through process No. 2 (b), process No. 3 (c), process No. 4 (d), process No. 5 (e) and process No. 6 (f).

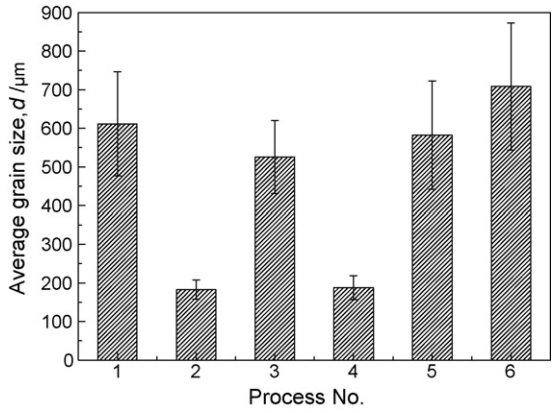

Fig. 2. Average grain sizes of the Mg–3%Al alloy treated through different processes.

4. Discussion

Significant grain refinement could be obtained for the Mg–3%Al alloy inoculated by carbon, as shown in Fig. 1a. For the refining mechanism of carbon inoculation, the hypothesis that Al_4C_3 particles formed by reaction between Al and C in the Mg–Al melt should act as nucleating substrates for Mg grains has been widely accepted by many researchers [5–10,12–18]. However, it should be noted that the Al–C–O particles have been always found in the Mg–Al alloys inoculated by carbon [5,6,12,13,16–18]. Likewise, the Al–C–O particles were also observed in the present study, as shown in Figs. 3 and 4. These Al–C–O particles should be actually the hydrolyzate of Al_4C_3 particles during specimen polishing, since Al_4C_3 is extremely reactive to water [12,16]. On the other hand, the formation of Al_2CO phase in the Mg melt is thermodynamically less favorable than the formation of Al_4C_3 phase [25].

The effect of Fe on the grain refinement of Mg–3%Al alloy, like the sample treated through process No. 3, has been discussed in the authors' previous study [24]. As for the Al–15%Fe master alloy

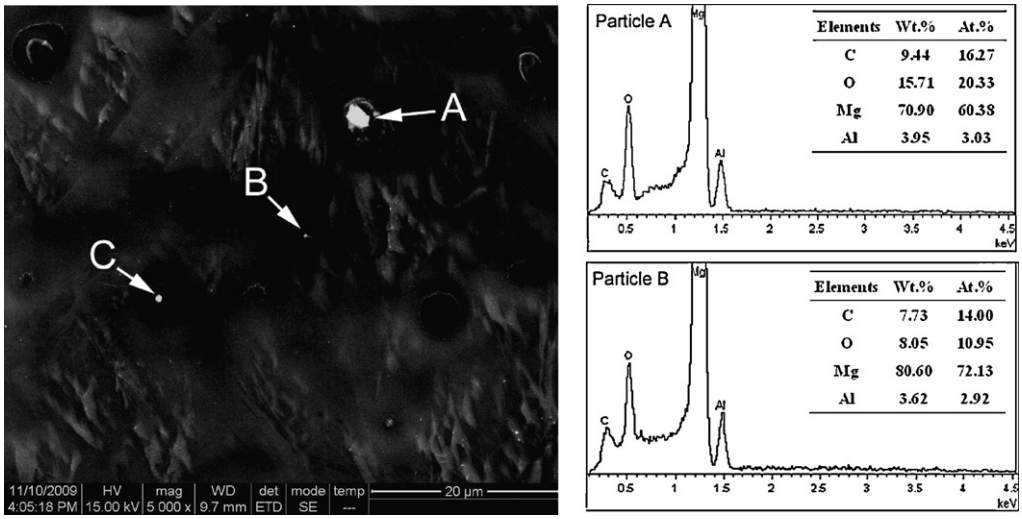

Fig. 3. SEM images of the Al–C–O particles in the Mg–3%Al alloy treated through process No. 2 and their typical EDS spectra measured from A and B particles.

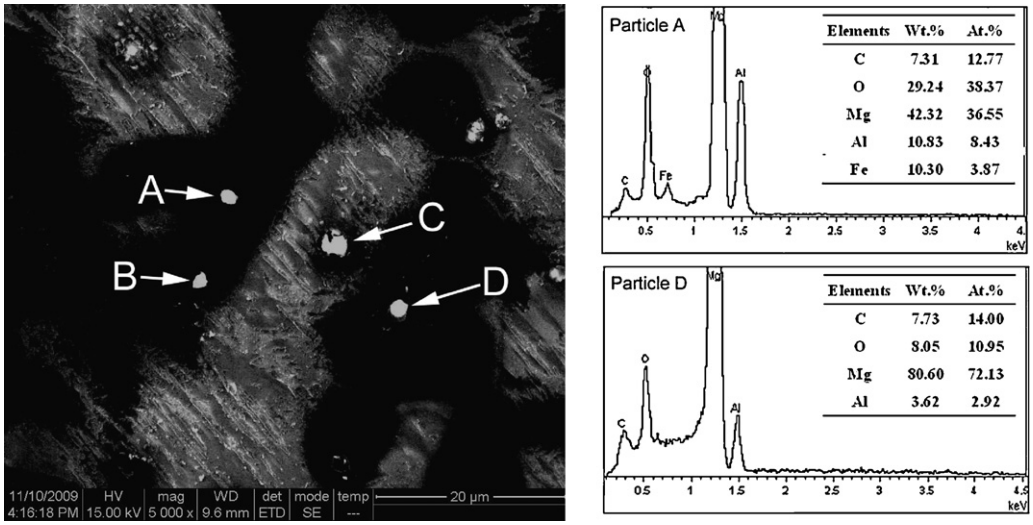

Fig. 4. SEM images of the Al–C–O–Fe particle (A) and the Al–C–O particles (from C to D) in the Mg–3%Al alloy treated through process No. 4 and their typical EDS spectra measured from A and D particles.

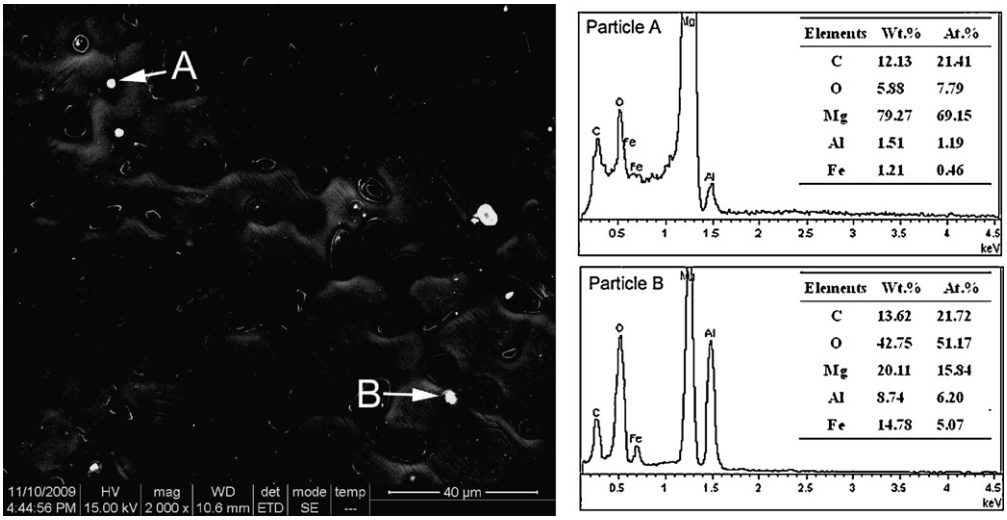

Fig. 5. SEM images of the Al–C–O–Fe particles in the Mg–3%Al alloy treated through process No. 5 and their typical EDS spectra measured from A and B particles.

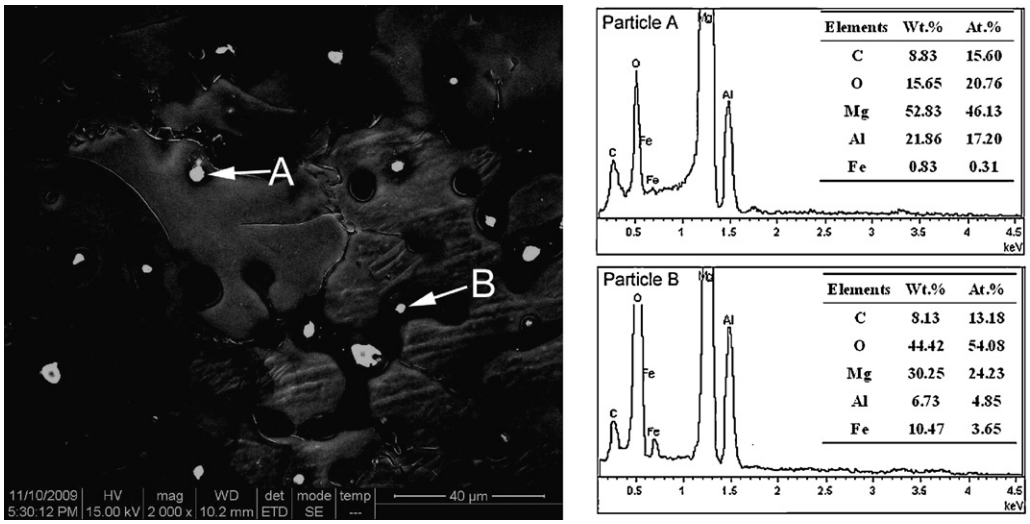

Fig. 6. SEM images of the Al–C–O–Fe particles in the Mg–3%Al alloy treated through process No. 6 and their typical EDS spectra measured from A and B particles.

used in the present study, its microstructure and X-ray diffraction (XRD) pattern are shown in Fig. 7. The element Fe mainly existed in the form of $AlFe_3$ and AlFe intermetallic compounds. Judged by Al–Fe binary phase diagram [26], the Al–15%Fe master alloy should consist of Al and Al_3Fe phases under equilibrium solidification. However, the AlFe phase is possibly formed in the Al–15%Fe master alloy under non-equilibrium solidification.

After the Al–15%Fe master alloy was added into the Mg–Al melt, some parts of Al–Fe intermetallic compounds were dissolved into the melt and the other parts remained in the melt since the Fe concentration in Mg melt is low (about 0.05% at 760 °C) [26]. Therefore, the element Fe in the Mg–Al melt should exist in the form of Al–Fe intermetallic compounds and solute Fe. As for the sample treated through process No. 4, the Al–15%Fe master alloy was added into the Mg–Al melt before being inoculated by carbon. Under this condition, the formation of Al_4C_3 was possibly interrupted by Al–Fe intermetallic compounds and solute Fe. Consequently, the Al–C–O–Fe particles could be observed in this sample, as the particles denoted by B to D in Fig. 4.

As far as the Al–C–O–Fe particles were concerned, they should be actually the Al–C–Fe-rich intermetallic compounds. These Al–C–Fe-rich compounds are possibly formed by the following processes. Firstly, the Al–C–Fe intermetallic compounds can be formed by a direct reaction among Al, C and Fe in the Mg–Al melt. Secondly, the Al–C compounds may be formed by a reaction between Al and C firstly, then the Al–C compounds are adsorbed on the surface of Al–Fe compounds. Thirdly, the Al–C–Fe compounds can be directly generated by a reaction between C and Al–Fe compounds on the surface. These processes may be competing with each other, resulting in the formation of Al–C–Fe compounds with different structures. Up to now, the structure of the Al–C–Fe intermetallic compounds formed by a direct reaction among Al, Fe and C in the magnesium melt has not been disclosed. So it is very difficult to judge whether these Al–C–Fe intermetallic particles can act as the nucleating substrates for Mg grains. However, as for the latter two ways, it is possible that the Al–C coating film is formed on the surface of the Al–Fe compounds.

As a result, the particles of Al–C–Fe compounds with duplex structures, *i.e.* an Al–C film on the Al–Fe compound, could possibly be formed. A hypothesis was firstly proposed by the present authors that an Al_4C_3 coating film could possibly be formed on the surface of some compounds with high melting-point [27]. Some powerful evidences have been provided to prove the validity of this hypothesis [17,28]. For example, the present authors found the duplex structures of the Al–C film on the Al_4Ca particles [17]. Liu et al. [28] found that an Al_4C_3 film could be formed on the Al–Mn intermetallic compounds.

These Al–C–Fe particles with an Al–C film should also act as nucleating substrates for Mg grains. The Al–C–Fe particles formed under this condition were theoretically proved to be potent nucleating substrates for Mg grains [24]. Therefore, the same refining efficiency could be obtained for the samples treated through pro-

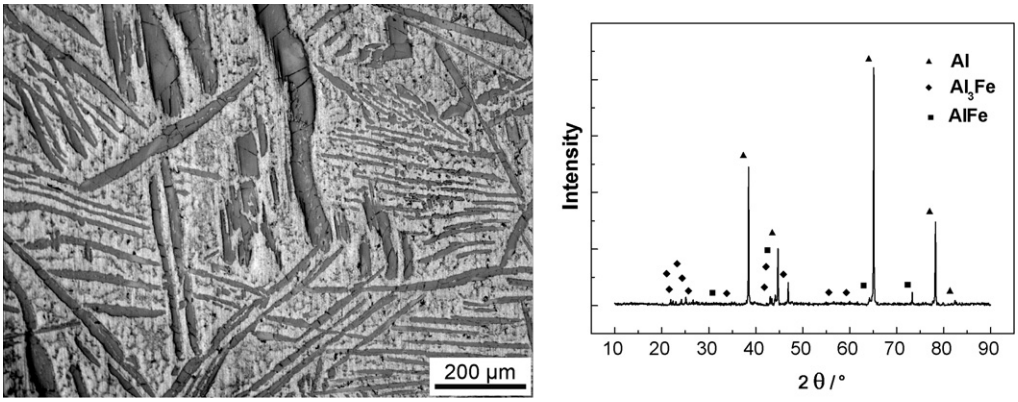

Fig. 7. Optical microstructure of the Al–15% Fe master alloy and its XRD pattern.

cess Nos. 2 and 4, since the two types of particles, *i.e.* Al–C particles and Al–C–Fe particles with Al–C film, could act as nucleating substrates for Mg grains.

However, the Al–C–O particles could hardly be found in the samples treated through processes Nos. 5 and 6. Only Al–C–O–Fe particles were observed in these two samples. They were also actually the Al–C–Fe-rich intermetallic compounds. For the process Nos. 5 and 6, the Al_4C_3 particles had already formed in the Mg–Al melt before Fe was added. Addition of Al-15%Fe master alloy was expected to introduce Al–Fe intermetallic compounds and a small amount of solute Fe into the Mg–Al melt. Many possibilities exist to form the Al–C–Fe particles, such as adsorption of Al_4C_3 and Al–Fe intermetallic particles, reaction of Al_4C_3 and solute Fe, as well as reaction of Al–Fe intermetallic particles and remaining carbon in the Mg–Al melt. Likewise, these processes may be competing with each other, resulting in the formation of Al–C–Fe compounds with different structures. The amount of the Al–C–Fe particles formed by reaction of Al–Fe phases and remaining carbon should be very low since the carbon concentration is very low (less than 20 ppm) in the Mg melt [14,26]. As for the first two situations, the particles of Al–C–Fe compound with duplex structures of an Al–Fe film on Al–C phase were possibly formed, resulting in poisoning of Al_4C_3 particles. In the study performed by Cao et al. [10], who attributed the poisoning effects of Fe and Mn to the formation of a coating film containing Fe and/or Mn on the Al_4C_3 nucleating particles.

Anyway, judged by the obvious grain coarsening for the two samples treated through processes Nos. 5 and 6, these Al–C–Fe particles should not be the potent nucleating substrates for Mg grains. Therefore, Fe played an inhibiting role in grain refinement of Mg–Al alloys inoculated by carbon under this condition, *i.e.* carbon inoculation before Fe addition. However, more careful microscopic works should be further carried out to understand the correlation between the crystal structures of the Al–C–Fe intermetallic compounds and the process conditions.

Based on the above discussion, it can be reasonably inferred that the Al–C–Fe particles with high content of Fe should be formed by the interaction of Al_4C_3 and Al–Fe intermetallic compounds. Under this condition, the Fe peaks in EDS spectra of the Al–C–Fe particles should be stronger, such as the particles denoted by A in Fig. 4, B both in Figs. 5 and 6. The Al–C–Fe particles with low content of Fe should be formed by reaction of Al, C and the solute of Fe in Mg melt, such as particle denoted by A in Fig. 6.

5. Conclusions

1. A significant grain refinement could be obtained for the Mg–3%Al alloy by carbon inoculation. That Fe inhibited the grain refinement or not was closely associated with the operating sequence of carbon inoculation and Fe addition.
2. Fe has no obvious effect on the grain refinement of Mg–3%Al alloy by carbon inoculation under the condition that Fe pre-existed in the Mg–Al melt before carbon inoculation. In contrast, Fe played an inhibiting role in the grain refinement of Mg–3%Al alloy by carbon inoculation under the condition that the Mg–Al melt was inoculated by carbon before Fe addition.
3. The Al–C–O particles were observed in the sample treated by carbon inoculation. In addition to the Al–C–O particles, the Al–C–O–Fe particles could be observed in the sample treated by Fe addition and then carbon inoculation. These Al–C–O and Al–C–O–Fe particles, actually being Al–C and Al–C–Fe phases, should be the potent nucleating substrates for Mg grains.
4. The Al–C–O–Fe-rich intermetallic particles were mainly observed in the samples treated by carbon inoculation before Fe addition. Under this condition, the Al–C–O–Fe particles, actually being Al–C–Fe phase, should not be the potent nucleating substrates for Mg grains.

Acknowledgement

This work is funded by National Science Foundation of China through project No. 50901034.

References

[1] B.L. Mordike, T. Ebert, Mater. Sci. Eng. A302 (2001) 37–45.
[2] A.A. Luo, Inter. Mater. Rev. 49 (2004) 13–30.
[3] J.D. Du, W.J. Han, Y.H. Peng, J. Cleaner Prod. 18 (2010) 112–119.
[4] X.Q. Zeng, Y.X. Wang, W.J. Ding, A.A. Luo, A.K. Sachdev, Metall. Mater. Trans. 37A (2006) 1333–1341.
[5] J. Du, J. Yang, M. Kuwabara, W.F. Li, J.H. Peng, Mater. Trans. 49 (2008) 2303–2309.
[6] Y.Q. Ma, R.S. Chen, E.H. Han, Mater. Lett. 61 (2007) 2527–2530.
[7] D.H. St. John, Q. Ma, M.A. Easton, C. Peng, Metall. Mater. Trans. A36 (2005) 1669–1679.
[8] Y.C. Lee, A.K. Dahle, D.H. St. John, Metall. Mater. Trans. A31 (2000) 2895–2906.
[9] T.I. Motegi, Mater. Sci. Eng. A413/414 (2005) 408–411.
[10] P. Cao, Q. Ma, D.H. St. John, Scr. Mater. 56 (2007) 633–636.
[11] P. Cao, Q. Ma, D.H. St. John, Scr. Mater. 51 (2004) 125–129.
[12] Y. Tamura, N. Kono, T. Motegi, E. Sato, J. Jpn. Inst. Light Met. 48 (1998) 395–399.
[13] Y. Tamura, E. Yano, T. Motegi, E. Sato, Mater. Trans. 44 (2003) 107–110.
[14] Q. Ma, C. Peng, Scr. Mater. 52 (2005) 415–419.
[15] Y.H. Liu, X.F. Liu, X.F. Bian, Mater. Lett. 58 (2004) 1282–1287.
[16] L. Lu, A. Kdahle, D.H. St. John, Scr. Mater. 53 (2005) 517–522.
[17] J. Du, J. Yang, M. Kuwabara, W.F. Li, J.H. Peng, J. Alloys Compd. 470 (2009) 134–140.
[18] J. Du, J. Yang, M. Kuwabara, W.F. Li, J.H. Peng, J. Alloys Compd. 470 (2009) 228–232.
[19] Q.L. Jin, J.P. Eom, S.G. Lim, W.W. Park, B.S. You, Scr. Mater. 49 (2003) 1129–1132.
[20] E.F. Emley, Principles of Magnesium Technology, Pregamom Press, Oxford, 1966, pp. 202–204.
[21] T. Haitani, Y. Tamura, E. Yano, T. Motegi, N. Kono, E. Sato, J. Jpn. Inst. Light Met. 51 (2001) 403–408.
[22] P. Cao, Q. Ma, D.H. St. John, Scr. Mater. 53 (2005) 841–844.
[23] Y.C. Pan, X.F. Liu, H. Yang, J. Mater. Sci. Technol. 21 (2005) 822–826.
[24] J. Du, J. Yang, M. Kuwabara, W.F. Li, J.H. Peng, Mater. Trans. 48 (2007) 2903–2908.
[25] Q.L. Jin, J.P. Eom, S.G. Lim, W.W. Park, B.S. You, Scr. Mater. 52 (2005) 421–423.
[26] T.B. Massalski, J.L. Murray, L.H. Bennett, H. Baker, Binary Alloy Phase Diagrams, American Society for Metals, Metals Park, OH, 1986.
[27] J. Du, J. Yang, M. Kuwabara, W.F. Li, J.H. Peng, Mater. Trans. 49 (2008) 139–143.
[28] S.F. Liu, Y. Zhang, H. Han, J. Alloys Compd. 491 (2010) 325–329.